Article published in Cerebral Cortex Advance Access (17th May 2006).

The original publication is available at http://cercor.oxfordjournals.org via the following DOI: http://dx.doi.org/10.1093/cercor/bhk034

Connectivity-Based Parcellation of Broca's Area

A. Anwander, M. Tittgemeyer, D.Y. von Cramon, A.D. Friederici, T.R. Knösche

Max Planck Institute for Human Cognitive and Brain Sciences, Leipzig, Germany

Corresponding author:

Dr. Marc Tittgemeyer

Max-Planck-Institute for Human Cognitive and Brain Sciences

Stephanstrasse 1a

04103 Leipzig, Germany

Tel.: +49 341 9940 229

Fax: +49 341 9940 221

Email: tittge@cbs.mpg.de

Submitted to Cerebral Cortex. *Pre-print: 31th August 2005.*

Abstract

It is generally agreed that the cerebral cortex can be segregated into structurally and functionally distinct areas. Anatomical subdivision of Broca's area has been achieved using different microanatomical criteria, such as cytoarchitecture and distribution of neuroreceptors. However, for the function of cortical areas, anatomical connectivity is most relevant. Hence, connectivity forms a sensible criterion for the functio-anatomical segregation of cortical areas. Diffusion-weighted MR imaging offers the opportunity to use this criterion in the individual living subject. Probabilistic tractographic methods provide excellent means to extract the connectivity signatures from these data sets. The correlations between these signatures are then used by an automatic clustering method to identify cortical regions with mutually distinct and internally homogeneous connectivity. We use this principle to parcellate Broca's area and to identify the typical connectivity patterns of putative BA44, BA45, and the deep frontal operculum. These results are discussed in the light of previous evidence from other methods in both human and non-human primates. We conclude that plausible results can be achieved by the proposed technique, which cannot be obtained by any other method *in vivo*. For the first time, there is a possibility to investigate the anatomical subdivision of Broca's area in the individual living human subject.

Key Words: diffusion imaging, tractography, cortex parcellation, Broca's area, connectivity

Introduction

It is widely accepted among neuroscientists that the cerebral cortex can be subdivided into a number of structurally and functionally distinct areas. This subdivision is referred to by the term *cortex parcellation* throughout this paper. Under the premise that structure reflects function, understanding the structural organisation of the cortex is vital for the study of brain function. However, what are the parameters that define a cortical area as structurally and functionally uniform and distinct from its neighbours?

Structural interpretations of functional imaging data are mostly based on the cytoarchitectonic map of Brodmann (1909), which reflects the specific variation in size and packing density of cell bodies across the depth profile of the cortical sheet in one single subject. Other parameters have been added successively, such as layering, distribution and amount of intracortical mylinated fibres (Vogt, 1910, 1911; Braitenberg, 1962) or the density of certain neurotransmitters receptors (Zilles et al., 2004). All these parameters describe the local microarchitecture of cortical tissue. However, as has been pointed out by Kaas (2002) and others (cf. Lanshley and Clark, 1946), differences between the microarchitectures of cortical areas are often subtle. In fact, it has been demonstrated that previously cyto- and myeloarchitectonically indistinguishable areas show a clear functional segregation (cf. Roland and Zilles, 1998; e.g. Friederici and Kotz, 2003, for the superior-posterior and the inferior portion of Brodmann area (BA) 44). Some of these functional segregations could be confirmed by receptorarchitectonic maps, e.g. the separation of BA44 into a dorsal and a ventral portion supporting phonological and syntactic processes, respectively (Friederici, 2002; Amunts and Zilles, in press). Furthermore, it has been argued that differences in input from and output to other brain areas may be a necessary additional criterion for the segregation of functionally different areas[1]. Hence, the pattern of anatomical connectivity[2] seems to be an important parameter for the description and distinction of cortical areas (cf. also Barbas and Rempel-Clower,

[1] In general, a subdivision based on more than one type of evidence would be more reliable (cf. van Essen, 1985; cf. Kaas, 1997).

[2] Within this article, we are limited to long-range connectivity, i.e. cortico-cortical association fibres, the cortico-spinal tract, transcallosal connections, etc. Intra-area connections or fibres between adjacent areas (u-fibres) are beyond the scope of this paper.

1997). This is particularly plausible in the understanding that higher cognitive functions are preferentially based on widespread networks, rather than isolated cortical areas. Therefore, the anatomical characterization of a particular cortical area just by its internal microstructure without regarding its connections to other brain areas must remain incomplete.

To date, connectivity information has been revealed mostly from animal models. They focus on the measurement of degenerating axons subsequent to lesion, or using active transport of tracers that are injected while the animal is still alive (Passingham et al., 2002). Though powerful, active axonal transport techniques have seen little or no application in human brain because they are limited to invasive studies of living tissue.

In principle, *post mortem* tracer application allows tracing of tracts too, in aldehyde-fixed (Haber, 1988) as well as in unfixed (McConnell et al., 1989) tissue, but only for distances of about 10 mm (Mufson et al., 1990). Longer distance connections can only be investigated by series of histological sections (Axer et al., 2002), dissection studies (Klingler and Gloor, 1960), or indirect evidence from anterograde degeneration due to brain lesions (DiVirgilio and Clarke, 1997). Due to these restrictions, information about long-range connectivity in the normal human has been difficult to obtain and is limited in scope (Clarke and Miklossy, 1990; Miklossy et al., 1991; Crick and Jones, 1993). With the advent of modern imaging technology, it has become possible to quantify long-range connectivity *in vivo* on the basis of diffusion-weighted magnetic resonance imaging (DW-MRI) using white matter tractography.

DW-MRI measures the direction-dependent mobility of water molecules (diffusion), which is influenced by the microscopic architecture of the brain tissue (Pierpaoli et al., 1996; Le Bihan et al., 2001; Beaulieu, 2002). Here, diffusion is measured in a number of directions, yielding an approximation of the 3D diffusivity profile in the respective voxel (typically containing a few cubic millimetres), which reflects direction-dependent (anisotropic) aspects of the tissue microstructure. Based on the diffusivity profile, several voxel-based metrics have been described, can be plotted throughout the brain, and highlight certain aspects of microstructure of both normal and pathological tissue (for a comprehensive review, see Tofts, 2004).

White matter tractography goes a step further. It attempts to integrate the local fibre orientation information by tracing the course of white matter fibre bundles throughout the

brain (for a review see Mori and van Zijl, 2002). Two major approaches are used to tackle this challenging task: deterministic and probabilistic tractography. Deterministic tractography produces maximum likelihood pathways through the diffusion weighted MR data set. These pathways are usually based on a 3D vector field comprising the principal eigenvectors of the diffusion tensors that are assumed to represent the main fibre direction in each voxel (Conturo et al., 1999; Mori et al., 1999; Basser et al., 2000; Poupon et al., 2000). Probabilistic approaches to the tractography problem take into account the uncertainty of the direction information in each voxel (Koch et al., 2002; Behrens et al., 2003b). Commencing at some seed voxel, tracking yields a probabilistic distribution of possibly connected voxels—the so-called *tractogram*. The basis for probabilistic tractography is the local probability density function generated by a mathematical model of the local diffusivity, e.g. the diffusion tensor model (Basser *et al.*, 1994). Here, each of the model parameters is characterized by a statistical distribution (e.g., expectation value and standard deviation of a normal distribution). In a second step the local probability density functions have to be connected using conditional probabilities.

The most straightforward application of tractography is the segmentation of the telencephalic white matter into compartments corresponding to the various systems of fibre bundles (Catani et al., 2002). The other obvious application concerns the degree of anatomical connectivity between different grey matter areas (Koch *et al.*, 2002; Behrens *et al.*, 2003b). Finally, if one seeks to subdivide brain structures according to their connectivity patterns, one can rely on the discriminative power of tractographic techniques. This has led to another powerful application of white matter tractography, namely connectivity-based cortex parcellation. The concept for a cortex parcellation based on tractography has been put forward by Johansen-Berg et al. (2004) and has been demonstrated to yield promising results for the medial frontal cortex (SMA/preSMA; Johansen-Berg *et al.*, 2004) and the geniculate bodies (Devlin et al., 2005).

In our study, we demonstrate that connectivity-based cortex parcellation is a suitable means to subdivide Broca's area, an area of high anatomical and functional complexity. For this purpose, we developed a technique, which combines a three-dimensional extension of the tractographic method of Koch et al. (2002) with some methodological concepts proposed by Johansen-Berg et al. (2004). To demonstrate the robustness of the

concept, we first replicated previous findings (parcellation of the medial frontal cortex). Then, we applied the method to Broca's area.

Broca's area resides in the inferior frontal cortex and traditionally comprises the lateral triangular and opercular portions of the inferior frontal gyrus (IFG). Here, also the cortical band between the crown of the opercular part of IFG and the anterior insula was included into the definition of Broca's area. We refer to this structure as *deep frontal operculum* (Fig. 1). It is well known that Broca's area can be structurally segregated using cytoarchitectonic methods (von Economo, 1929; Sanides, 1962, 1966; Amunts et al., 1999; Amunts and Willmes, 2005; Amunts and Zilles, in press)[3] or receptor mapping (Zilles et al., 2002; Amunts and Zilles, in press). However, *in vivo* separation in individual subjects has not yet been achieved. We hypothesize that the subregions of Broca's area are distinct not only in their microanatomy, but also in their pattern of long-range connectivity. Thus, connectivity based parcellation would offer the possibility to define their borders in the *individual living subject* on the basis of structural, rather than macroanatomical (gyri and sulci) criteria.

[3] Dysgranular BA44 (roughly corresponding to opercular IFG), granular BA45 (roughly corresponding to triangular IFG), and agranular deep frontal operculum.

Methods

Data acquisition and pre-processing

Diffusion weighted data and high-resolution 3-dimensional (3D) T1 weighted as well as 2-dimensional T2 weighted images were acquired in 6 healthy right-handed subjects (28 ± 3 years; 3 females) on a Siemens 3T Trio Scanner with an 8-channel array head coil and maximum gradient strength of 40 mT/m. The diffusion weighted data were acquired using spin-echo echo planar imaging (TR=8100 ms, TE=120 ms, 44 axial slices, resolution 1.7×1.7×3.0 mm, 10 % gap, 2 acquisitions). Written informed consent was obtained from all subjects in accordance with the ethical approval from the University of Leipzig. The diffusion weighting was isotropically distributed along 24 directions (b-value=1000 s/mm^2). Additionally, a data set with no diffusion weighting was acquired. The high angular resolution of the diffusion weighting directions improves the robustness of probability density estimation (see below) by increasing the signal-to-noise ratio per unit time and reducing directional bias. The total scan time for the DWI protocol was approximately 7 minutes.

As first step in pre-processing the data, the 3D T1 weighted (MPRAGE; TR=100 ms, TI=500 ms, TE=2.96 ms, resolution 1.0×1.0×1.0 mm, flip angle 10°, 2 acquisitions) images were reoriented to the plane of anterior and posterior commissure. Upon reorientation, the T2 weighted images (RARE; TR=7800 ms, TE=105 ms, 44 axial slices, resolution 0.7×0.7×3.0 mm, 10% gap, flip angle 150°) were co-registered to the reoriented 3D T1 weighted images according to a "mutual information" registration scheme (Studholme et al., 1997). Subsequently, by using in-house software (Wollny and Kruggel, 2002) the DWI- EPI images were non-linearly warped onto the T2 weighted images to reduce distortion artefacts. Following correction of image distortion, the diffusion tensor was calculated for each voxel using multivariate linear regression after logarithmic transformation of the signal intensities (Basser *et al.*, 1994). The fractional anisotropy (FA) of the tensor in each voxel was subsequently determined, and a multislice fractional anisotropy image (Basser and Pierpaoli, 1996) was created.

For presentation purposes, on basis of the T1 weighted images cortical surfaces have been rendered by using Freesurfer (Dale et al., 1999).

Definition of the Regions of Interest

Regions of interest (ROIs) for the white matter tractography in each subject were defined by an expert (DYvC) on the basis of individual T1 weighted MR images. They encompassed parts of the left inferior frontal cortex, i.e. the deep frontal operculum as well as the surface portion of the opercular and triangular part of the inferior frontal gyrus (Fig. 1). The ROIs were segmented into white and grey matter compartments thresholding the fractional anisotropy (white matter: FA > 0.15). Each white matter voxel in the region of interest that neighboured a grey matter voxel was labelled as a seed voxel for the tractographic procedure (Fig. 2).

White Matter Tractography

We developed a 3 dimensional extension of the random walk method proposed by Koch et al. (2002). The algorithm was applied to each of the seed voxels. The target space was the whole white matter volume with a resolution of $1.0 \times 1.0 \times 1.0$ mm^3. The algorithm can be described by a model of randomly moving particles. Imagine a particle in a seed voxel **A**, moving in a random manner from voxel to voxel. The transition probability to a neighbouring voxel depends on the local probability density function (lPDF) based on the local diffusivity profile that is modelled from the DTI measurement. This lPDF is discretised into 26 directions corresponding to neighbouring voxels and yields higher transitional probabilities along directions with high diffusivity, i.e. the presumed fibre directions. Hence, the particle will move with a higher probability along a fibre direction than perpendicular to it. If we perform this 'experiment' many times and count how often particles from voxel **A** reach a target voxel **B**, we obtain a relative measure of the anatomical connectivity between the two voxels. The random walk is stopped when the particle leaves the white matter volume. The 3-dimensional distribution of the connectivity values of a particular seed voxel with all voxels in the brain is called a *tractogram*. The average tractogram for an entire region we call the *connectivity signature* of this region.

For each elementary transition of the particle, the probability for a movement from the seed voxel *m* to the target voxel *n* (the lPDF) is computed as

$$P(m \to n) = (d_{m \to n,m} \cdot d_{m \to n,n})^a$$

$P(m \to n)$: probability for a transition from voxel *m* to voxel *n*,

$d_{m \to n,m}$: diffusion coefficient in voxel *m* for the direction of the connecting line between voxel *m* and *n*.

The exponent $a=7$ is used to focus the probability distribution to main fibre direction and suppress the influence of the transverse diffusion. The value was empirically chosen in such a way that the trajectories of most particles follow the main fibre directions as defined by the lPDF. The transition directions in the local model are limited to the 26 discrete neighbours of the voxel, which is sufficient to produce a smooth distribution of the fibres directions after interpolation of the tensor data to 1 mm voxel size. A total of 100000 particles were tested for each seed voxel. To compensate for the distance dependent bias, each connectivity value is normalized to the shortest pathway between the seed and the respective target voxel. After reducing the dynamic range of the connectivity values by logarithmic transformation, the values were scaled to the maximum value in the seed voxel. To remove random artefacts, only connectivity values bigger than 0.4 were used for further processing.

Cortex parcellation

The idea behind cortex parcellation is that cortex areas with similar long-range connectivity are combined into a region, which is segregated from neighbouring regions with different connectivity. The connectivity pattern of a cortical voxel is approximated by the tractogram associated to its neighbouring white matter voxel. The general principle of the parcellation technique is illustrated in Fig. 2. For each seed voxel within a ROI, a tractogram was computed. The correlation values between any two of these tractograms were computed and arranged in the *connectivity correlation matrix*. The i^{th} column or row in this symmetric matrix characterizes the degree of similarity between the tractogram of seed voxel *i* and all other seed voxels. Consequently, the very high dimensional space of tractograms (dimension: number of with voxels in the white matter) is transformed to a lower dimensional space of tractogram similarity patterns (dimension: number of seed

voxels in the region of interest). It is immediately plausible that voxels with similar connectivity patterns (i.e. tractograms) show also a similar pattern of correlation with the tractograms belonging to other seed voxels (i.e. similar columns in the connectivity correlation matrix). In order to define collections of voxels with similar connectivity, a multidimensional k-means cluster algorithm was applied to the columns of the connectivity correlation matrix. Like for any clustering method, one pitfall is the trade-off between model consistency (how well does the clustering describe the structure of the data) and model complexity (preference of a simple model that describes the relevant features and ignores noise), with the consequence that the number of clusters has to be introduced from outside. Therefore different numbers of clusters can be tested. We accepted only those solutions that were consistent across subjects, i.e. the principal arrangement of the areas associated with the clusters was the same. Moreover, each area had to represent a connected region of the cortex. Finally, every area was additionally characterized by its connectivity signature[4].

To demonstrate the robustness of connectivity-based cortex parcellation, the method was applied to the same region as investigated in the work of Johansen-Berg et al. (2004) – the medial frontal cortex. A separation along the AC line into an anterior and a posterior part was found (Fig. 3A), which corresponds exactly with the findings of Johansen-Berg et al. (2004). Increasing the number of clusters, the region was divided posterior-anteriorly into 3 areas. They presumably represent preSMA, SMA, and M1. Both the most anterior (preSMA) and the most posterior (M1) regions could be separated between the hemispheres, while the middle one (SMA) could not be split, even if the number of clusters was increased further (Fig. 3B). Most importantly, the separation between preSMA and SMA remained at the AC line. The connectivity signatures for the different areas demonstrate the correspondence in connectivity between the left and right hemisphere areas, caused by strong transcallosal connections (Fig. 3C). As also found by Johansen-Berg et al. (2004), the posterior areas predominantly exhibit connections to premotor/motor regions and the cortico-spinal tract, while the anterior area seems to be more connected to prefrontal and parietal regions. We conclude that the replication of the

[4] Connectivity signature: average tractogram for a certain region.

results by Johansen-Berg et al. (2004) with a different method documents the robustness of this kind of approach to cortex parcellation.

Results

In all 6 cases, the method revealed a clear segregation of Broca's area into the surface portion of BA44/45 and the deep frontal operculum (Fig. 4). Additionally, in 5 subjects the surface portion split along the ascending branch of the lateral sulcus into a rostral and a caudal part, suggesting a separation between BA44 and BA45. In the remaining data set (subject III), the clustering algorithm left the surface portion of the IFG undivided. In subject I, the ventralmost portion of the triangular part forms a common region together with the deep frontal operculum. A similar effect is observed in subject III for the posterior convexity of the orbital part of the IFG.

The connectivity signatures of the deep frontal operculum show projections through the anterior subinsular white matter and the inferior level of the external capsule to the temporal isthmus. From there, connection can be further traced to the anterior temporal lobe, into the inferior occipito-frontal fascicle, as well as into the inferior longitudinal fascicle. Moreover, a second more inferior (ventral) pathway follows the uncinate fascicle in lateral direction into the anterior temporal lobe in all but one subject. Medially this pathway can be tract into the basal forebrain, i.e. into the amygdala complex and into the septal region. In two subjects, there are additional connections to the frontopolar cortex (BA10).

Putative BA44 and BA45 show the same connections through the inferior external capsule as found for the deep frontal operculum. Additionally, a more superior (dorsal) pathway exhibits connections to the parietal lobe and towards the perisylvian region via the superior longitudinal ("arcuate") fascicle (in 4 subjects) as well as in all subjects to the dorsomedial prefrontal cortex and to the ventral portion of precentral gyrus. In the signatures of BA44, the arcuate fascicle is more dominant, while for BA45 there are stronger connections with the dorsomedial prefrontal cortex and through the external capsule. For the signatures of a typical subject (subject I), refer to Fig. 5.

Discussion

Methodological Issues

As reasoned in the introduction and evidenced by our findings, long-range connectivity is a functio-anatomically relevant trait of the brain. It is therefore a suitable criterion for the identification of mutually distinct cortical areas. Yet, it is not clear to what extent diffusion based white matter tractography reflect the fine details of anatomical connectivity[5].

Resolution in the Region of Interest

The proposed parcellation method relies to the differentiation of tractograms associated to all voxels included in the region of interest. However, the limited spatial resolution of the measurement essentially restricts the differentiability of adjacent tractograms. Figure 6 illustrates the relationship between anatomical structures and DT-MRI voxel resolution. DT-MRI can image these structures only incompletely: (1) structure is not observed directly, but only by hindrance of water diffusion; (2) the dimensions of these structures (in the order of microns) are far beyond the resolution currently available to MR based techniques (in the order of millimetres) and cannot be resolved by tractography; (3) the method is not suited to whether, how often, or in what direction action potentials travel along the identified pathways. Any tractographic result is based on the integrative effect of a large number of microscopic structures, including neural and glial tissue. Cortical voxels integrate information of structures oriented in many different directions, and therefore do not exhibit much net anisotropy[6]. Directly underneath the cortical layers, there is the layer of u-fibres (about 0.75-1 mm thick, cf. Rockland, 1989), which is connecting neighbouring cortical areas. Only beyond this u-fibre belt, the actual long-range fibre bundles are sufficiently dominant to determine the direction of the gross diffusion within a voxel. Therefore, the seed points for our DTI tractography algorithm resides below the u-fibres making sure that the computed connectivity signatures are

[5] This also implies the question for the comparability with connectivity data obtained by alternative techniques, e.g. tracer studies.

[6] This is true for current DTI resolution, which cannot resolve e.g. the Baillarger stripes, see de Crespigny (2005).

dominated by long-range connections. In contrast, Johansen-Berg et al. (2004) used both cortical and sub-cortical seed voxels. However, starting the tracking procedure in grey matter will allow the pathways to make detours over the neighbouring cortical voxels, the transition to which is (almost) equally probable as to white matter fibre bundles. This might result in an additional loss of resolution.

However, even when seeding in the sub-cortical white matter, resolution is limited. DTI voxels sizes are currently in the order of 2-3 millimetres (Fig. 6). Hence, relatively few potential tractography seed voxels reside within a gyrus. Consequently, they bear just an approximate relationship to the cortex. Additionally, they may be subject to partial volume effects from u-fibres, resulting in similar tractograms for neighbouring areas connected by u-fibres.

Tracking Artefacts

The precise relation between DTI based tractography findings and the underlying microstructure remains unclear. The exact modelling of this relationship would be immensely complex and has not yet been accomplished. Moreover, even if such a model would exist, its inversion (i.e. the reconstruction of the microstructure from the DTI data) is an underdetermined problem with no unique solution. Hence, some of the identified connections might just be artefacts of the method. A major source of such tracking artefacts is created by close contact between parallel or crossing fibre bundles, causing the main fibre directions in the respective voxels to be poorly defined (Wiegell et al., 2000; Barrick and Clark, 2004). Strategies to combat this uncertainty have been proposed (for a review, see Mori and van Zijl, 2002). However, there is no way to reconstruct information, which is not contained in the measured data. Therefore, instead of trying to resolve the irresolvable, one can quantify the uncertainty using probabilistic methods (Koch *et al.*, 2002; Behrens *et al.*, 2003b). This is the approach we followed in this work. It avoids systematic biases to a certain extent and instead introduces a quantification of uncertainty, where a clear decision on the propagation direction is impossible. We therefore did not obtain one solution, as with deterministic tractography, but the so-called tractogram, which is a collection of possibly connected brain areas, weighted by their probability. An exact probabilistic (Bayesian) solution for tracking was proposed by Behrens et al. (2003a; 2003b). However, the accuracy of this global approach depends on

the local model linking the fibre direction distribution to the measured diffusion profile. Since such local models are currently still quite imperfect, this global solution cannot unfold its full potential yet. Therefore, we opted for a more heuristic approach, similar to the one proposed by Koch et al. (2002). In particular, the strong decay of the connectivity values with increasing distance from the seed voxel was counterbalanced by normalization to the path length. Therewith, a disproportional influence of the shorter-range connectivity onto the correlations between the tractograms was avoided.

From above, one can conclude that the tractograms reflect anatomical connectivity only in an indirect way. However, for the purpose of cortex parcellation, not the connectivity itself, but its difference between areas is important. Hence, even not completely plausible tractograms can yield a correct parcellation result. It is certainly possible that also connectivity differences are eradicated by the described artefacts. Then, areas with different connectivity patterns are not distinguishable by their tractograms any more. On the other hand, established differences between tractograms – as we found them between the subregions within the IFG – allow the conclusion that there is also different connectivity.

Parcellation

Once the tractograms have been computed for every seed voxel in the region of interest, it remains to be decided, which of them are similar enough to be clustered together in one area. This is essentially a modelling process. We seek to describe a real situation, where in fact every seed voxel is associated with a different tractogram (i.e. with a simplified model). As with any model, there are the opposing demands for describing the data accurately (accounting for as much variance as possible) and effectively (with as few parameters as possible) at the same time. Once we have opted for a certain level of model complexity (i.e. the number of areas), we need to assign the seed voxels to these areas (i.e. determining the area boundaries) as objectively and reproducibly as possible. For this task, Johansen-Berg et al. (2004) chose a method, based on visual subdivision of the re-ordered correlation matrix of the tractograms. We replaced this approach by an automatic clustering algorithm. This gave us a more objective way to assign seed voxels (i.e. tractograms) to the areas, once we have decided on the number of clusters.

Yet, the decision on the number of clusters is not easy to make. There might even be several correct choices, i.e. several levels of parcellation. Hierarchical clustering methods could make a contribution here. The decision, which number(s) of areas describe the data better than others, could possibly be tackled by the use of information criteria, which attempt an information-theoretically founded optimal compromise between model complexity and model accuracy (see e.g. Knösche et al., 1998).

Anatomical Issues

So far, structural subdivisions of inferior frontal cortex (IFC) were only available from *post mortem* specimens. In living subjects, they had to be identified indirectly by macroanatomical landmarks. However, there is an unreliable association of these landmarks with cytoarchitectonically defined borders of cortical areas (Zilles et al., 1997; Geyer et al., 1999; Amunts et al., 2000; Geyer et al., 2000; Grefkes et al., 2001), in particular in the IFC (Amunts et al., 1999; Amunts et al., 2004).

We have shown that tractography based cortex parcellation can reliably segregate putative BA44 from the deep frontal operculum (Fig. 4). Moreover, in all but one case, also the separation between putative BA44 and BA45 could be found along the chosen macroanatomical boundary (i.e. the ascending branch of the lateral fissure). In the remaining case (subject III), only one area, covering both the opercular and triangular parts of the IFG, could be identified. However, the most anterior portion in this case was classified by its connectivity signature as putative BA45. This means that in this case the boundary between BA44 and BA45 is located more anterior than macroanatomy would suggest. In another case (subject I), the most anterior portion of the triangular part is separated from putative BA45. It is characterized by a connectivity signature similar to the one attributed to the deep frontal operculum. We propose that in this case the border between BA45 and BA47 is more posterior than macroanatomical landmarks (i.e. anterior branch of the lateral sulcus) would suggest. This proposal is paralleled by the macaque literature (Pandya and Yeterian, 1996; Romanski et al., 1999a; Petrides and Pandya, 2002), which indicates that area 47/12 is strongly connected to brain regions in much the same way as were our findings for the deep frontal operculum. The finding in subject III seems to support this, too: Here, the posterior portion of the orbital part of IFG is

separated from the triangular part along the anterior branch of the lateral sulcus and appears to have a very similar connectivity signature as the deep frontal operculum.

The connectivity signatures for the IFG in general let us to deduce three principal pathways: (1) a dorsal one via the arcuate fascicle, (2) a middle one through the inferior external capsule, and (3) a ventral one via the uncinate fascicle.

The dorsal pathway connects several parietal and temporal (superior and middle temporal gyrus) association cortices, which is largely in line with findings from monkey tracer studies (Pandya and Yeterian, 1996; Romanski et al., 1999b; Petrides and Pandya, 2002) as well as with MRI based white matter parcellation in humans (Makris et al., 1999; Mori et al., 2005). However, the projections into the anterior middle temporal gyrus are not supported by these studies but appear to be present in other DTI inferences of the arcuate fascicle (e.g., Catani et al., 2005). This might be caused by an artefact of tractographic methods due to close contact of fibres (so-called "kissing" fibres, see above). In accordance with literature, the dorsal pathway via the arcuate fascicle particularly connects BA44 and –in our case to a somewhat lesser extent– BA45 with parietal and temporal association cortices (Parker et al., 2005; Pulvermuller, 2005).

The middle pathway was found for all three areas. It appears to connect the IFG with the superior temporal lobe. Connections to the inferior longitudinal fascicle and the posterior section of the inferior fronto-occipital fascicle – i.e. projections into the occipital lobe – are less plausible and could be again due to a methodological artefact. In particular, for putative BA45 the appearance of a dorsal and a middle pathway would be in line with a further distinction between an anterior and a posterior portion (BA45A/B, Petrides and Pandya, 1994; Petrides and Pandya, 2002). We speculate that the dorsal pathway is attributed to BA45B –and that the connectivity pattern of this region would be more BA44 alike– whereas the middle pathway rather connects BA45A with the anterior temporal lobe.

The ventral pathway connects the deep frontal operculum with the anterior temporal lobe. It has to be pointed out that the uncinate and inferior occipito-frontal fibre bundles are certainly impossible to be disentangled given the current DTI resolution and the very close intertwinement of the two fibre systems[7]. The actual anatomical connectivity may

[7] For particularly instructive illustrations and an extensive description of the anatomical complexity of the brain's fibre systems, see Dejerine (1895).

therefore include either of the fibre systems or both. Especially the uncinate fascicle has very strong connections to constituents of the basal forebrain, in particular to the amygdala complex and the septal area (Ebeling and von Cramon, 1992). It is interesting that the deep frontal operculum is connected to structures of the limbic system. Therefore, its anatomical connectivity appears to be similar to that of BA47(/12), but rather different from the surface portion of Broca's area, BA44 and BA45. This is particularly interesting in the light of Friederici and colleague's finding that the deep frontal operculum may support the processing of a more primitive type of grammar, whereas the surface portion of Broca's area subserves the processing of a more complex grammar (Friederici et al., 2005).

Resume

We have presented a method for the segregation of cortical areas in the individual living subject. This method is based on probabilistic tractography and relies on diffusion-weighted MRI data. The replication of the previous results by Johansen-Berg et al. (2004) provided confidence in this kind of parcellation technique. Using this method, we have segregated three regions of Broca's area. This segregation was found to be plausible in the light of previous microanatomical and functional findings. Putatively, the found regions represent BA44 and BA45 as well as the deep frontal operculum. We conclude that the proposed method for cortex parcellation seems capable of revealing aspects of the functio-anatomical organisation of the cortex that are not possible to obtain by other methods in the individual living subject. Additionally, we argue that the tractographic results are useful not only for the differentiation between cortical areas, but also for the characterization of long-range connectivity itself. The dominant connections for the studied areas are summarized in Fig. 7.

Acknowledgements

The authors wish to thank S. Kotz and J. Derfuss for fruitful discussions on our findings, H. Schmidt and S. Seifert for help with the figures and segmentation of the ROIs, respectively, as well as M. Brass for his part in the initiation of this project.

Bibliography

Amunts K, Malikovic A, Mohlberg H, Schormann T, Zilles K (2000) Brodmann's areas 17 and 18 brought into stereotaxic space - Where and how variable? Neuroimage 11: 66-84.

Amunts K, Schleicher A, Burgel U, Mohlberg H, Uylings HB, Zilles K (1999) Broca's region revisited: cytoarchitecture and intersubject variability. J Comp Neurol 412: 319-341.

Amunts K, Weiss PH, Mohlberg H, Pieperhoff P, Eickhoff S, Gurd JM, Marshall JC, Shah NJ, Fink GR, Zilles K (2004) Analysis of neural mechanisms underlying verbal fluency in cytoarchitectonically defined stereotaxic space - The roles of Brodmann areas 44 and 45. Neuroimage 22: 42-56.

Amunts K, Willmes K (2005) From intersubject variability in clinical syndromes to anatomical variability. Brain Lang.

Amunts K, Zilles K (in press) A multimodal analysis of structure and function in Broca's region. In: Broca's Region (Grodzinski Y, Amunts K, eds.). Oxford: Oxford University Press.

Axer H, Leunert M, Murkoster M, Grassel D, Larsen L, Griffin LD, von Keyserlingk DG (2002) A 3D fiber model of the human brainstem. Comput Med Imag Grap 26: 439-444.

Barbas H, Rempel-Clower N (1997) Cortical structure predicts the pattern of corticocortical connections. Cerebral Cortex 7: 635-646.

Barrick TR, Clark CA (2004) Singularities in diffusion tensor fields and their relevance in white matter fiber tractography. Neuroimage 22: 481-491.

Basser PJ, Mattiello J, LeBihan D (1994) Estimation of the effective self-diffusion tensor from the NMR spin echo. J Magn Reson B 103: 247-254.

Basser PJ, Pajevic S, Pierpaoli C, Duda J, Aldroubi A (2000) In vivo fiber tractography using DT-MRI data. Magn Reson Med 44: 625-632.

Basser PJ, Pierpaoli C (1996) Microstructural and physiological features of tissues elucidated by quantitative-diffusion-tensor MRI. J Magn Reson B 111: 209-219.

Beaulieu C (2002) The basis of anisotropic water diffusion in the nervous system - a technical review. NMR Biomed 15: 435-455.

Behrens TE, Johansen-Berg H, Woolrich MW, Smith SM, Wheeler-Kingshott CA, Boulby PA, Barker GJ, Sillery EL, Sheehan K, Ciccarelli O, Thompson AJ, Brady JM, Matthews PM (2003a) Non-invasive mapping of connections between human thalamus and cortex using diffusion imaging. Nat Neurosci 6: 750-757.

Behrens TE, Woolrich MW, Jenkinson M, Johansen-Berg H, Nunes RG, Clare S, Matthews PM, Brady JM, Smith SM (2003b) Characterization and propagation of uncertainty in diffusion-weighted MR imaging. Magn Reson Med 50: 1077-1088.

Braitenberg V (1962) A note on myeloarchitectonics. J Comp Neurol 118: 141-156.

Brodmann K (1909) Vergleichende Lokalisationslehre der Großhirnrinde in ihren Prinzipien dargestellt auf Grund des Zellaufbaues. Leipzig: Barth.

Catani M, Howard RJ, Pajevic S, Jones DK (2002) Virtual in vivo interactive dissection of white matter fasciculi in the human brain. Neuroimage 17: 77-94.

Catani M, Jones DK, Ffytche DH (2005) Perisylvian language networks of the human brain. 57: 8-16.

Clarke S, Miklossy J (1990) Occipital cortex in man: organization of callosal connections, related myelo- and cytoarchitecture, and putative boundaries of functional visual areas. J Comp Neurol 298: 188-214.

Conturo TE, Lori NF, Cull TS, Akbudak E, Snyder AZ, Shimony JS, McKinstry RC, Burton H, Raichle ME (1999) Tracking neuronal fiber pathways in the living human brain. Proc Natl Acad Sci U S A 96: 10422-10427.

Crick F, Jones E (1993) Backwardness of human neuroanatomy. Nature 361: 109-110.

Dale AM, Fischl B, Sereno MI (1999) Cortical surface-based analysis. I. Segmentation and surface reconstruction. Neuroimage 9: 179-194.

de Crespigny A (2005) Is there any value in studying diffusion anisotropy in the cortex? In: ISMRM Workshop on Quantative Diffusion Imaging. Lake Louise: Interantional Society for Magnetic Resonance in Medicine.

Dejerine J (1895) Anatomie des Centre Nerveaux. Paris: Rueff et Cie.

Devlin J, Sillery E, Johansen-Berg H, Behrens T, Matthews PM, Hall D, Moore D (2005) Identification of the auditory thalamus using multi-modal structural analyses. In: (Zilles K, Poline J-B, Grady C, eds.) 11th Anual Meeting of the Organisation for Human Brain Mapping. Toronto: Elsevier.

DiVirgilio G, Clarke S (1997) Direct interhemispheric visual input to human speech areas. Hum Brain Mapp 5: 347-354.

Ebeling U, von Cramon DY (1992) Topography of the Uncinate Fascicle and Adjacent Temporal Fiber Tracts. Acta Neurochir 115: 143-148.

Friederici AD (2002) Towards a neural basis of auditory sentence processing. Trends Cogn Sci 6: 78-84.

Friederici AD, Bahlmann J, Heim S, Schubotz RI (2005) The brain differentiates human and non-human grammar. submitted.

Friederici AD, Kotz SA (2003) The brain basis of syntactic processes: functional imaging and lesion studies. Neuroimage 20 Suppl 1: S8-17.

Geyer S, Schleicher A, Zilles K (1999) Areas 3a, 3b, and 1 of human primary somatosensory cortex 1. Microstructural organization and interindividual variability. Neuroimage 10: 63-83.

Geyer S, Schormann T, Mohlerg H, Zilles K (2000) Areas 3a, 3b, and 1 of human primary somatosensory cortex - 2. Spatial normalization to standard anatomical space. Neuroimage 11: 684-696.

Grefkes C, Geyer S, Schormann T, Roland P, Zilles K (2001) Human somatosensory area 2: Observer-independent cytoarchitectonic mapping, interindividual variability, and population map. Neuroimage 14: 617-631.

Haber S (1988) Tracing Intrinsic Fiber-Connections in Postmortem Human-Brain with Wga-Hrp. Journal of Neuroscience Methods 23: 15-22.

Johansen-Berg H, Behrens TE, Robson MD, Drobnjak I, Rushworth MF, Brady JM, Smith SM, Higham DJ, Matthews PM (2004) Changes in connectivity profiles define functionally distinct regions in human medial frontal cortex. Proc Natl Acad Sci U S A 101: 13335-13340.

Kaas JH (1997) Theories of visual cortex organisation in primates. In: Cereral Cortex (Rockland KS, Kaas JH, Peters A, eds.), pp 91-125. New York: Plenum Press.

Kaas JH (2002) Cortical Areas and Patterns of Cortico-Cortical Connections. In: Cortical Areas: Unity and Diversity (Schütz A, Miller R, eds.), pp 179-191. London: Taylor & Francis.

Klingler J, Gloor P (1960) The Connections of the Amygdala and of the Anterior Temporal Cortex in the Human Brain. Journal of Comparative Neurology 115: 333-&.

Knösche TR, Berends EM, Jagers HRA, Peters MJ (1998) Determining the number of independent sources of the EEG: A simulation study on information criteria. Brain Topogr 11: 111-124.

Koch MA, Norris DG, Hund-Georgiadis M (2002) An investigation of functional and anatomical connectivity using magnetic resonance imaging. Neuroimage 16: 241-250.

Lanshley KS, Clark G (1946) The cytoarchitecture of the cerebral cortex of Ateles: A critical examinantion of architectonic studies. J Comp Neurol 85: 223-306.

Le Bihan D, Mangin JF, Poupon C, Clark CA, Pappata S, Molko N, Chabriat H (2001) Diffusion tensor imaging: concepts and applications. J Magn Reson Imaging 13: 534-546.

Makris N, Meyer JW, Bates JF, Yeterian EH, Kennedy DN, Caviness VS (1999) MRI-Based topographic parcellation of human cerebral white matter and nuclei II. Rationale and applications with systematics of cerebral connectivity. Neuroimage 9: 18-45.

McConnell SK, Ghosh A, Shatz CJ (1989) Subplate Neurons Pioneer the 1St Axon Pathway from the Cerebral-Cortex. Science 245: 978-982.

Miklossy J, Clarke S, Van der Loos H (1991) The long distance effects of brain lesions: visualization of axonal pathways and their terminations in the human brain by the Nauta method. J Neuropathol Exp Neurol 50: 595-614.

Mori S, Crain BJ, Chacko VP, van Zijl PC (1999) Three-dimensional tracking of axonal projections in the brain by magnetic resonance imaging. Ann Neurol 45: 265-269.

Mori S, van Zijl PC (2002) Fiber tracking: principles and strategies - a technical review. NMR Biomed 15: 468-480.

Mori S, Wakana S, Nagae-Poetscher LM, van Zijl PCM (2005) MRI Atlas ofHuman White Matter. Amsterdam: Elsevier.

Mufson EJ, Brady DR, Kordower JH (1990) Tracing Neuronal Connections in Postmortem Human Hippocampal Complex with the Carbocyanine Dye Dii. Neurobiol Aging 11: 649-653.

Pandya DN, Yeterian EH (1996) Comparison of prefrontal architecture and connections. Philos T Roy Soc B 351: 1423-1432.

Parker GJM, Luzzi S, Alexander DC, Wheeler-Kingshott CAM, Clecarelli O, Ralph MAL (2005) Lateralization of ventral and dorsal auditory-language pathways in the human brain. Neuroimage 24: 656-666.

Passingham RE, Stephan KE, Kotter R (2002) The anatomical basis of functional localization in the cortex. Nature Reviews Neuroscience 3: 606-616.

Petrides M, Pandya DN (1994) Comparative cytoarchitectonic analysis of the human and the macaque frontal cortex. In: Handbook of Neuropsychology (Boller F, Grafman J, eds.), pp 17-58. Amsterdam: Elsevier.

Petrides M, Pandya DN (2002) Comparative cytoarchitectonic analysis of the human and the macaque ventrolateral prefrontal cortex and corticocortical connection patterns in the monkey. Eur J Neurosci 16: 291-310.

Pierpaoli C, Jezzard P, Basser PJ, Barnett A, Di Chiro G (1996) Diffusion tensor MR imaging of the human brain. Radiology 201: 637-648.

Poupon C, Clark CA, Frouin V, Regis J, Bloch I, Le Bihan D, Mangin J (2000) Regularization of diffusion-based direction maps for the tracking of brain white matter fascicles. Neuroimage 12: 184-195.

Pulvermuller F (2005) Opinion: Brain mechanisms linking language and action. Nat Rev Neurosci 6: 576-582.

Rockland KS (1989) Bistratified Distribution of Terminal Arbors of Individual Axons Projecting from Area-V1 to Middle Temporal Area (Mt) in the Macaque Monkey. Visual Neurosci 3: 155-170.

Roland PE, Zilles K (1998) Structural divisions and functional fields in the human cerebral cortex. Brain Res Brain Res Rev 26: 87-105.

Romanski LM, Bates JF, Goldman-Rakic PS (1999a) Auditory belt and parabelt projections to the prefrontal cortex in the rhesus monkey. J Comp Neurol 403: 141-157.

Romanski LM, Tian B, Fritz J, Mishkin M, Goldman-Rakic PS, Rauschecker JP (1999b) Dual streams of auditory afferents target multiple domains in the primate prefrontal cortex. Nat Neurosci 2: 1131-1136.

Sanides F (1962) Die Architektonik des menschlichen Strinhirns. Berlin: Springer.

Sanides F (1966) Architecture of Human Frontal Lobe and Relation to Its Functional Differentiation. Int J Neurol 5: 247-&.

Studholme C, Hill DL, Hawkes DJ (1997) Automated three-dimensional registration of magnetic resonance and positron emission tomography brain images by multiresolution optimization of voxel similarity measures. Med Phys 24: 25-35.

Tofts P, ed. 2004. Quantitative MRI of the Brain. Chinchester: Wiley & Sons.

van Essen DC (1985) Functional organisation of primate visual cortex. In: Cerebral Cortex (Peters A, Jones EG, eds.), pp 256-329: New York.

Vogt O (1910) Die myeloarchitektonische Felderung des menschlichen Stirnhirns. Journal für Psychologie und Neurologie 15: 221-232.

Vogt O (1911) Die Myeloarchitektonic des Isocortex parietalis. Journal für Psychologie und Neurologie 18: 379-390.

von Economo C (1929) The cytoarchitectonics of the human cerebral cortex. London: Oxford University Press.

Wiegell MR, Larsson HB, Wedeen VJ (2000) Fiber crossing in human brain depicted with diffusion tensor MR imaging. Radiology 217: 897-903.

Wollny G, Kruggel F (2002) Computional cost of nonrigid registration algorithms based on fluid dynamics. IEEE Trans Med Imaging 21: 946-952.

Zilles K, Palomero-Gallagher N, Schleicher A (2004) Transmitter receptors and functional anatomy of the cerebral cortex. J Anat 205: 417-432.

Zilles K, Schleicher A, Langemann C, Amunts K, Morosan P, PalomeroGallagher N, Schormann T, Mohlberg H, Burgel U, Steinmetz H, Schlaug G, Roland PE (1997) Quantitative analysis of sulci in the human cerebral cortex: Development, regional heterogeneity, gender difference, asymmetry, intersubject variability and cortical architecture. Hum Brain Mapp 5: 218-221.

Zilles K, Schleicher A, Palomero-Gallagher N, Amunts K (2002) Quantitative analysis of cyto- and receptorarchitecture of the human brain. In: Brain Mapping: The Methods (Mazziotta JC, Toga A, eds.). San Diego: Elsevier.

Figure Captions

Figure 1: Definition of the region of interest at the example of subject I. On the cortex convexity, only the opercular and triangular parts of the inferior frontal gyrus are visible. The deep portion of frontal operculum (cortical band between the lateral opercular part of IFG and the anterior insula) is indicated in the sagittal slice.

Figure 2: General methodology of connectivity based cortex parcellation. Seed voxels in white matter near the white-grey-matter-interface (WGMI), form the region of interest (A). For each of these voxels, a tractogram is computed (B). The matrix containing the correlations between all these tractograms is divided into clusters of voxels with similar correlation to other voxels (C). Each of these clusters corresponds to a certain area on the WGMI (D).

Figure 3: Parcellation of the medial frontal cortex in one subject (subject II, in the later applications). A and B: Color coded areas are projected onto the medial surfaces of the left and right hemispheres. A: Two clusters divide the area along the AC line into an anterior and a posterior part. B: Five clusters separate between the hemispheres, leaving one common area just posterior to the AC line. C: Connectivity signatures of the areas shown in B, viewed from the mid-sagittal plane.

Figure 4: Parcellation results for the inferior frontal cortex into three clusters for 6 subjects plotted on the Talairach scaled cortical surfaces. Insets show axial slices at three different levels that equidistantly cut through the parcelated areas.

Figure 5: Parcellation and signatures of the left inferior frontal cortex for a representative subject.

Figure 6: Illustration of typical DTI resolution (2.5 mm) in relation to anatomical structures of the temporal lobe. In particular, u- fibres are sketched in green and the long association fibres in blue.

Figure 7: Schematic representation of the principal connections found for the studied areas. Red: deep frontal operculum. Light green: BA44. Blue: BA45. Dark green: ventral PCG. Purple: dorsal PCG.

Figure 1

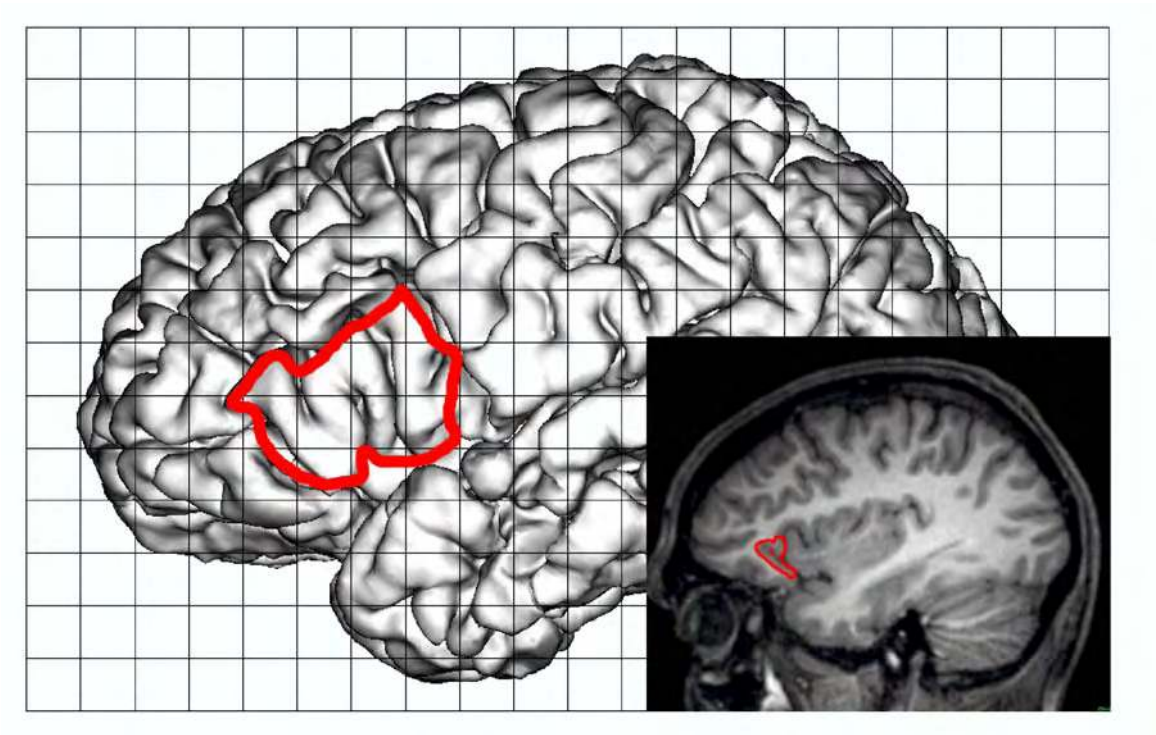

Figure 2

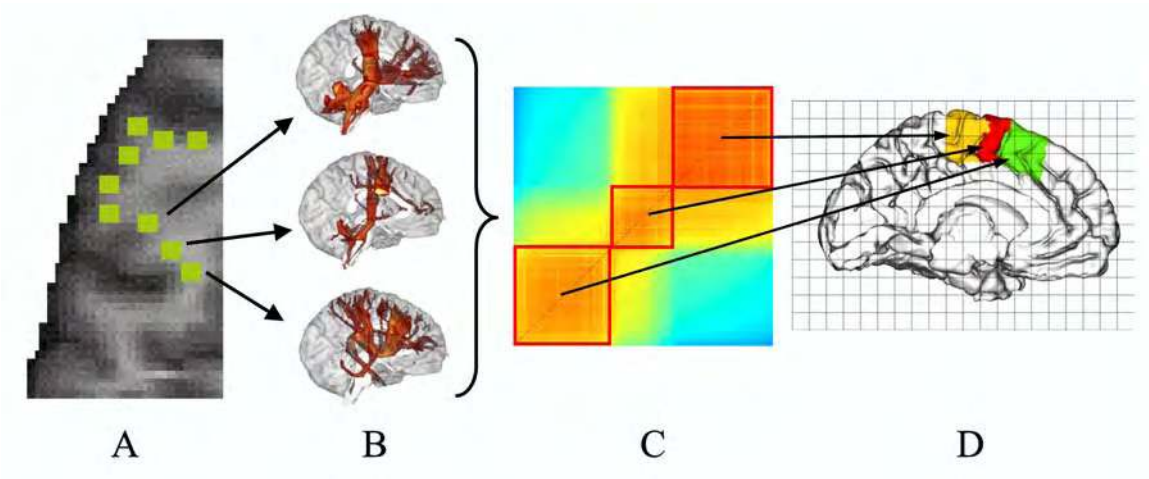

Figure 3

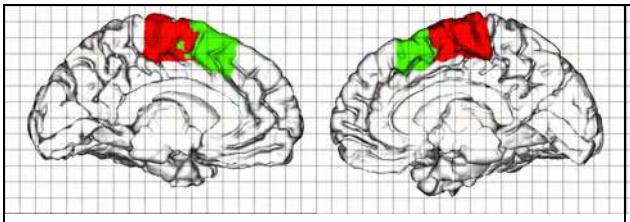

A: Parcellation of Medial Fontal Cortex into two areas, putative SMA including M1 (red) and preSMA (green)

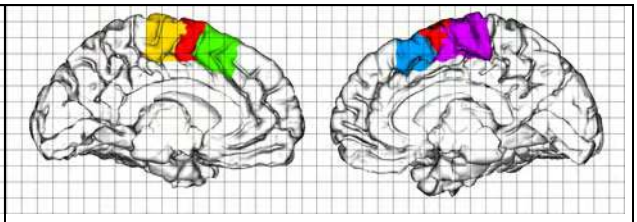

B: Parcellation into five areas: left/right M1 (yellow/purple), left/right preSMA (green/blue), centre area, probably SMA (red)

C: Signatures of areas in B

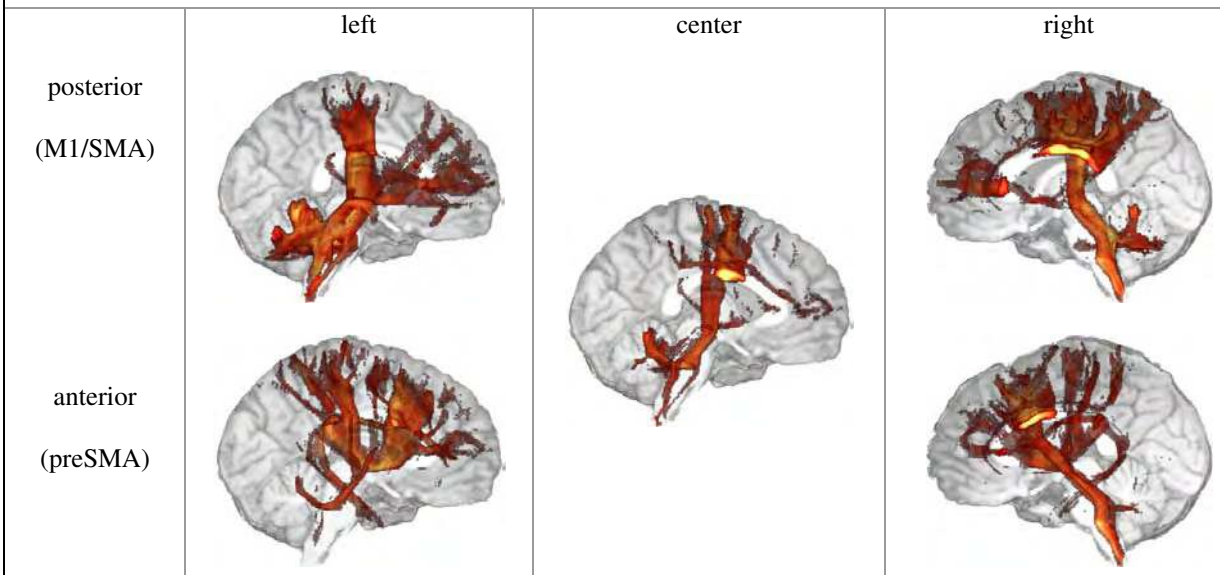

Figure 4

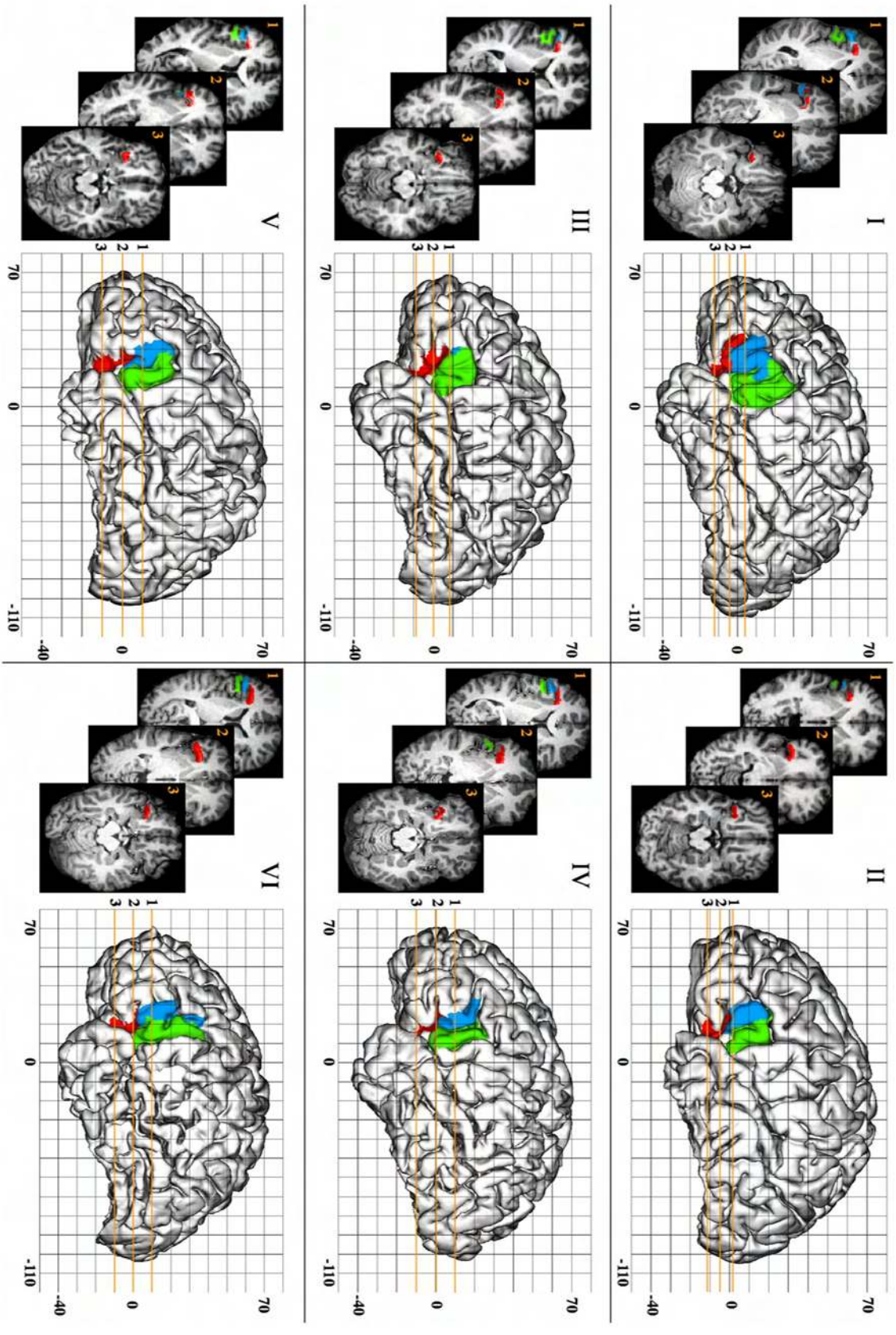

Figure 5

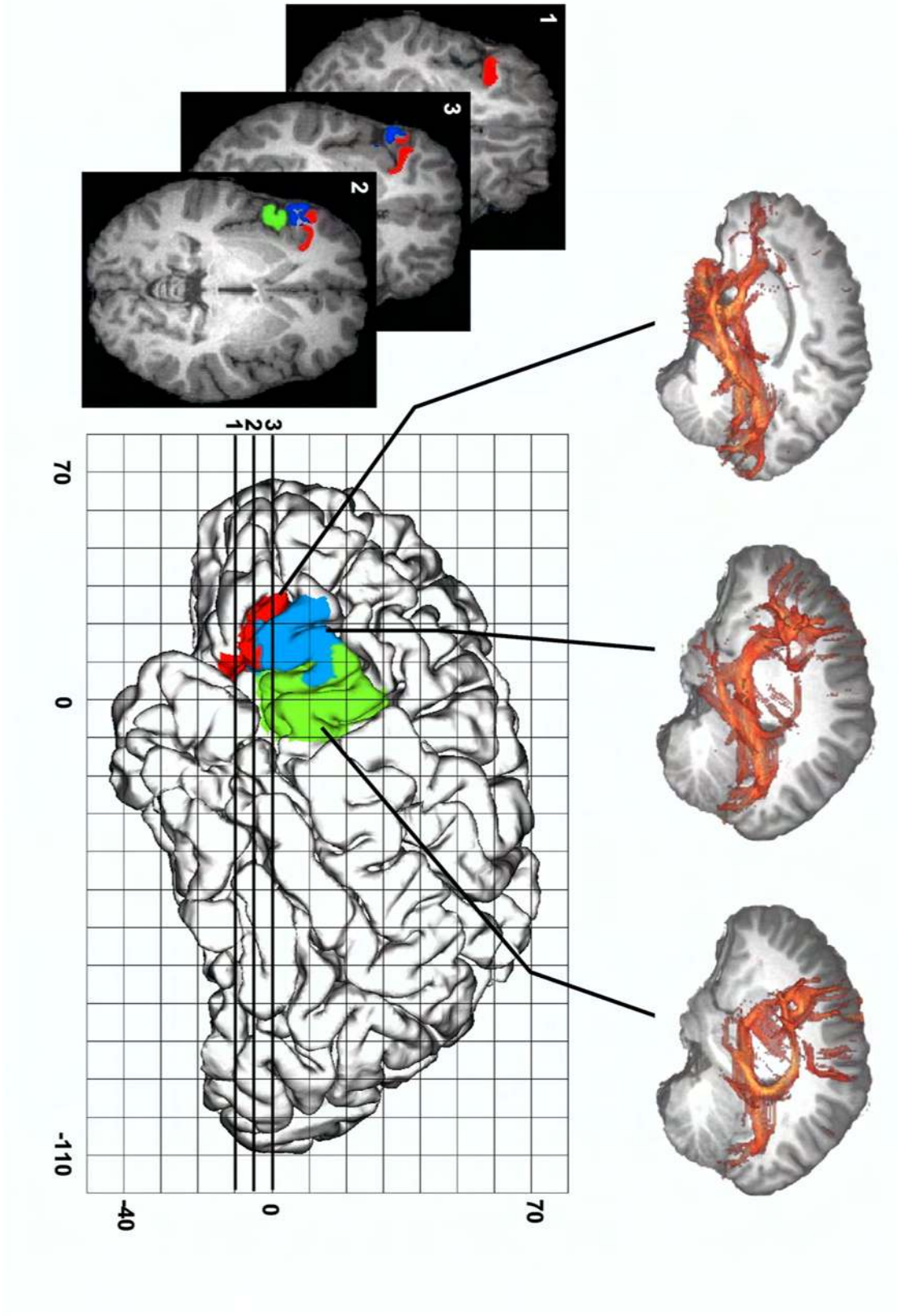

Figure 6

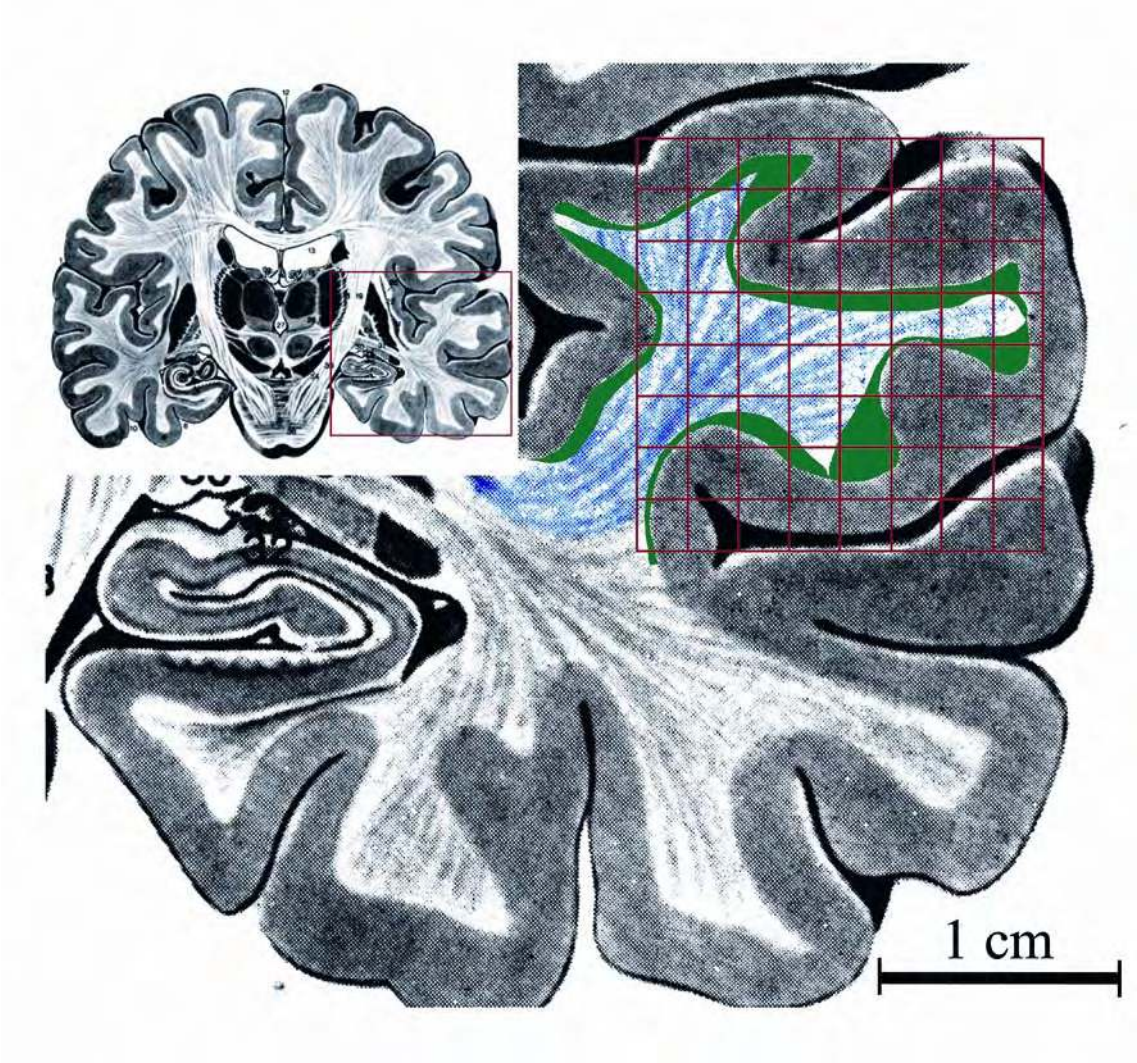

Figure 7